Supplementary Information

Few-layered titanium trisulfide (TiS_3) field-effect transistors

Alexey Lipatov,[a] Peter M. Wilson,[a] Mikhail Shekhirev,[a] Jacob D. Teeter,[a] Ross Netusil,[a] and Alexander Sinitskii*[a,b]

[a]*Department of Chemistry, University of Nebraska – Lincoln, Lincoln, NE 68588, USA*

[b]*Nebraska Center for Materials and Nanoscience, University of Nebraska – Lincoln, Lincoln, NE 68588, USA*

***E-mail:** *sinitskii@unl.edu*

Contents

1. Experimental Details

1.1. Materials

Ti foil (99.99+%, thickness ~ 0.25 mm) was received from Alfa Aesar. Sulfur (99.5+%) was received from Sigma-Aldrich. Heavily doped p-type silicon wafers covered with 300 ± 15 nm thick SiO_2 were received from Silicon Quest International.

For electron-beam lithography we used PMMA950 A4 (4% polymethyl methacrylate in anisole, MicroChem Corp.), methyl isobutyl ketone : isopropanol (1:3) (MIBK:IPA, MicroChem Corp.), isopropanol (99.5+%, Sigma-Aldrich), and acetone (99.7%, Fisher Scientific).

For electron-beam deposition we used chromium (Cr, 99.999%) and gold (Au, 99.999%), both of which were received from International Advanced Materials.

For atomic layer deposition we used trimethylaluminum (98%, Strem Chemicals) and nanopure water (18.2 MΩ·cm resistivity at 25 ºC).

1.2. Methods

Single-Crystal X-Ray Diffraction (XRD). X-ray intensity data was collected on a Bruker Smart Apex single-crystal diffractometer equipped with a Smart Apex CCD area detector and a graphite-monochromated MoKα radiation (λ = 0.071073 nm). Orientation matrix and unit cell parameters were derived using APEX2 software (Bruker (2007) APEX2, 2011.4-1; Bruker AXS Inc.: Madison, Wisconsin, USA, 2011)

Device fabrication. PMMA was spin-coated on the Si/SiO_2 substrates with TiS_3 nanoribbons at 5000 rpm for 45 sec. The wafers were then placed on a hotplate at 180 °C for 120 sec and cooled for 1 min. A Zeiss Supra 40 Field-Emission Scanning Electron Microscope and a Raith Pattern Generator were used to pattern electrodes on TiS_3 nanoribbons using electron-beam lithography. The substrates were then developed using MIBK:IPA mixture for 60 sec, rinsed with isopropanol, and dried with nitrogen gas. An AJA E-beam system was used to evaporate chromium at 0.2 Å/sec until a thickness of 3 nm (measured by a quartz crystal microbalance) was achieved. Cr evaporation was followed immediately by evaporation of 20 nm of gold at 0.5 Å/sec. The liftoff treatment to remove PMMA and excess metals consisted of submerging samples in hot acetone for 5 min, rinsing with isopropanol and then water, and drying with nitrogen gas.

Atomic layer deposition (ALD). The ALD process was carried out for 280 cycles at a temperature of 150 °C using a Fiji 200 ALD reactor from Cambridge Nanotech Inc. Trimethylaluminum and nanopure water were each pulsed at 60 msec, with each pulse followed by a 30 sec purge time. This procedure resulted in an Al_2O_3 dielectric layer of about 30 nm in thickness.

Atomic Force Microscopy (AFM). All AFM images were collected in a tapping mode using a Digital Instruments Nanoscope IIIa Dimension 3100 scanning probe microscope. The AFM data were analyzed using Nanoscope Analysis software.

Scanning Electron Microscopy (SEM). SEM was performed using a Zeiss Supra 40 Field-Emission Scanning Electron Microscope at an accelerating voltage of 5 kV.

Electrical measurements. Electrical measurements were performed using a Lake Shore TTPX cryogenic probe station at the base pressure of $\sim 1\times10^{-6}$ Torr. The device electrodes were connected to an Agilent 4155C semiconductor parameter analyzer that was linked to a computer through 82357B USB/GPIB interface and controlled using a National Instruments LabView code. In all measurements the drain-source voltage was $V_{DS} = 0.1$ V.

Raman spectroscopy. Raman spectra were recorded using a Thermo Scientific DXR Raman microscope with a 532 nm laser.

2. XRD results

Table S1: X-Ray single crystal data at room temperature for TiS_3 single crystal.

Nominal composition	TiS_3
Calculated density (g/cm^3)	3.30
Source radiation, nm	Mo*Kα*; 0.071073
Space group	*P 2$_1$/m (No 11)*
Pearson symbol	*mP8*
a (nm)	0.4948(7)
b (nm)	0.3379(5)
c (nm)	0.8748(12)
β (°)	97.62(2)
Cell volume (nm^3)	0.1449(14)
Formula units	Z = 2
Structure prototype	$ZrSe_3$
Index range	$-6 \leq h \leq 5$
Index range	$-4 \leq k \leq 4$
	$-11 \leq l \leq 11$
Reflections in refinement	$435 \geq 3\sigma(I_o)$ of 702
Number of variables	21
$R_F^2 = \Sigma\|F_0^2-F_c^2\|/\Sigma F_0^2$	0.125
wR^2	0.146
GOF	2.13

Table S2: Atomic and anisotropic displacement parameters for TiS_3

Atom	Wyckoff position	x	y	z	Anisotropic displacement (Å^2)		
					U_{11}	U_{22}	U_{33}
Ti1	2e	0.2872(9)	1/4	0.1510(4)	0.0088(19)	0.005(2)	0.023(2)
S1	2e	0.4614(12)	1/4	0.025(3)	0.025(3)	0.010(3)	0.002(2)
S2	2e	0.7601(11)	1/4	0.0514(6)	0.007(3)	0.005(3)	0.018(2)
S3	2e	0.8883(11)	1/4	0.6730(5)	0.011(2)	0.006(3)	0.0010(19)

$U_{12} = U_{13} = U_{23} = 0$

These data can also be accessed in a CIF file that is provided separately.

3. Additional SEM characterization of TiS_3 whiskers

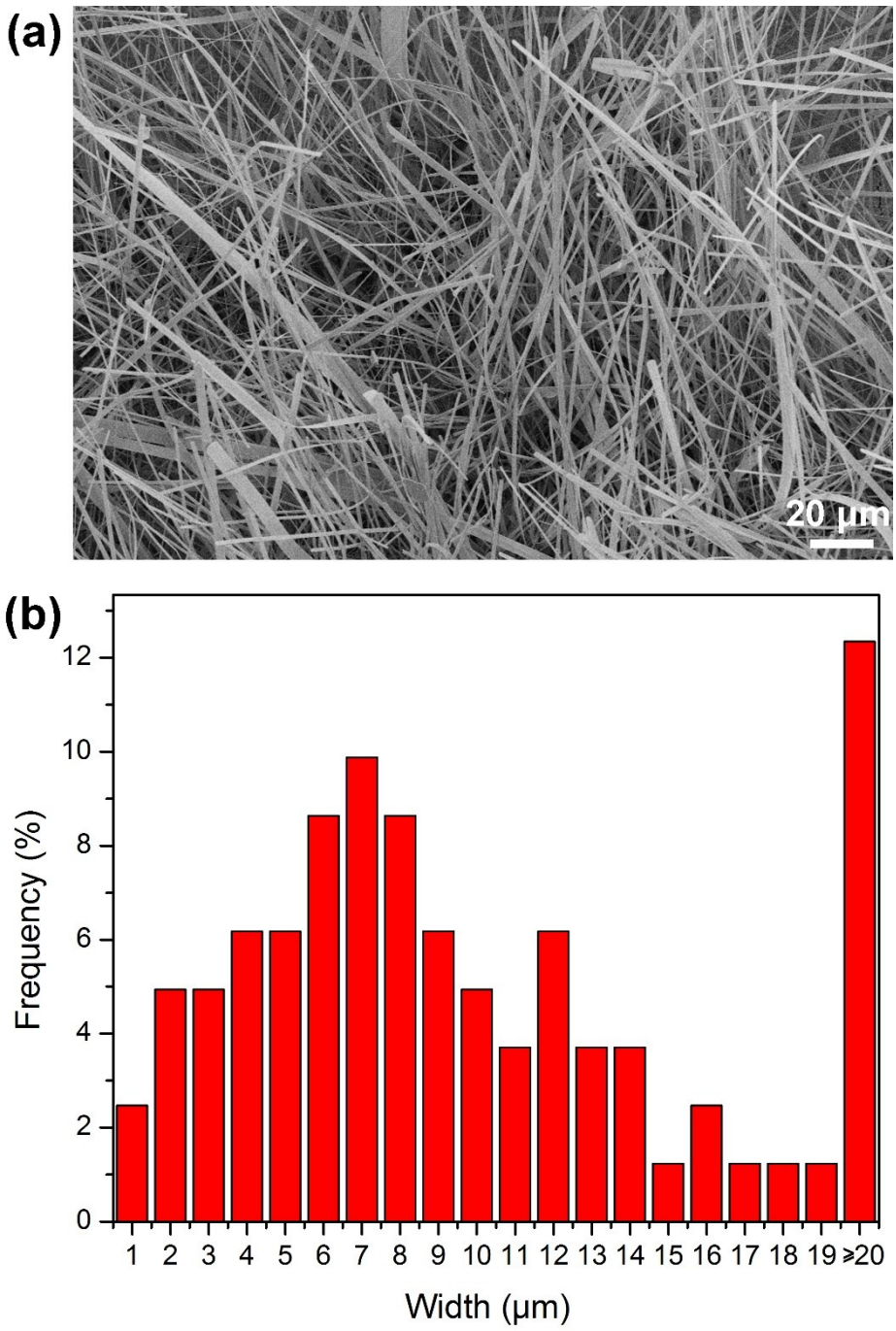

Figure S1. (a) SEM image of TiS_3 whiskers. **(b)** Width distribution of TiS_3 whiskers based on SEM image shown in (a) and similar SEM images.

4. Raman spectroscopy

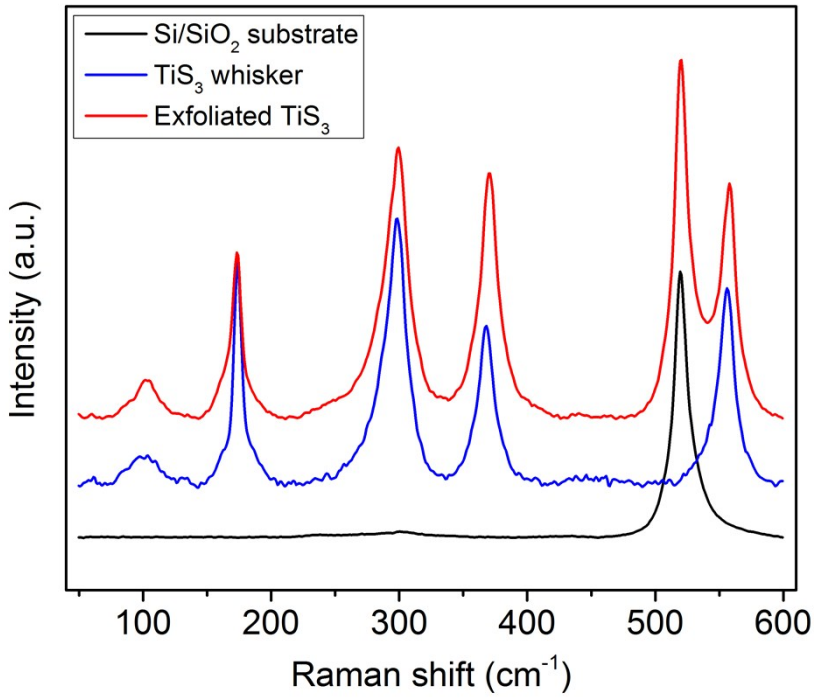

Figure S2. Raman spectra of a free-standing TiS_3 whisker (blue) and a 4-nm-thick exfoliated TiS_3 flake on Si/SiO_2 substrate (red). Raman spectrum of Si/SiO_2 substrate (black) is shown as a reference.

5. Microscopic characterization of TiS_3 FETs

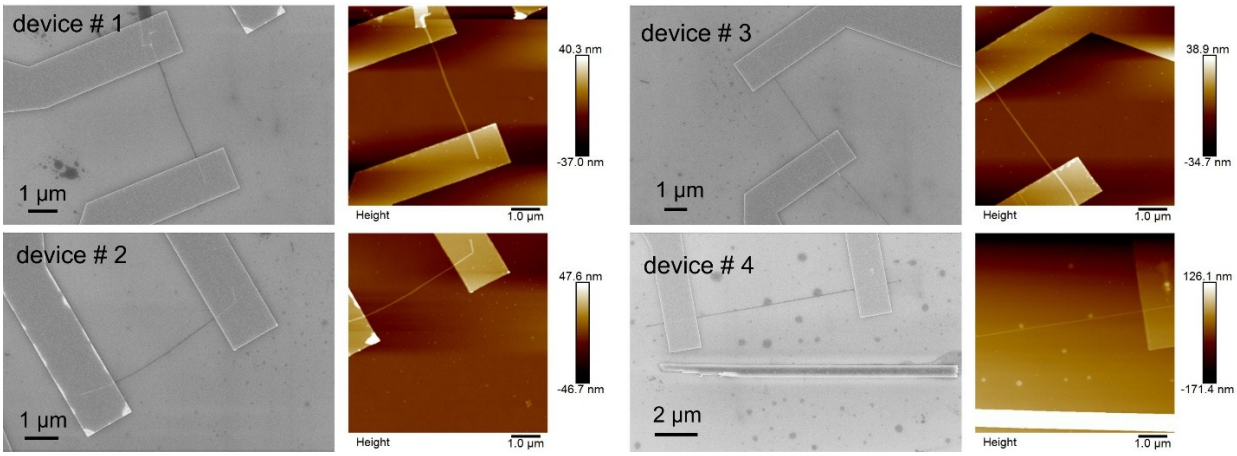

Figure S3. SEM and AFM images of few-layer TiS_3 FETs that were fabricated and tested in this study.

6. Four-point probe measurements

We fabricated two multi-terminal TiS_3 devices that are shown in Figures S4a and S5a. Each device is based on a single exfoliated TiS_3 nanoribbon that bridges four Cr/Au electrodes. For this device configuration we needed TiS_3 flakes that were at least 20 µm long, which were generally thicker and wider than shorter TiS_3 flakes that were used for the fabrication of two-terminal devices reported in this study (see Figures 2 and S3). As demonstrated by the AFM data presented in Figures S4b,c and S5b,c, the TiS_3 ribbons used for the contact resistance measurements had widths of 0.17 and 0.32 µm, respectively, and were less than 40 nm thick. Figures S4d and S5d show conductivity (σ) – gate voltage (V_G) dependences that were measured using a four-point probe method. The calculated field-effect mobilities, 21.1 and 24.2 $cm^2V^{-1}s^{-1}$, are comparable to the values measured for two-terminal devices (Figure 2e). Because of the substantial thickness of long TiS_3 nanoribbons, and thus their high conductivity, the ON/OFF ratios of these devices were very low, so these devices were not used for Al_2O_3 ALD experiments.

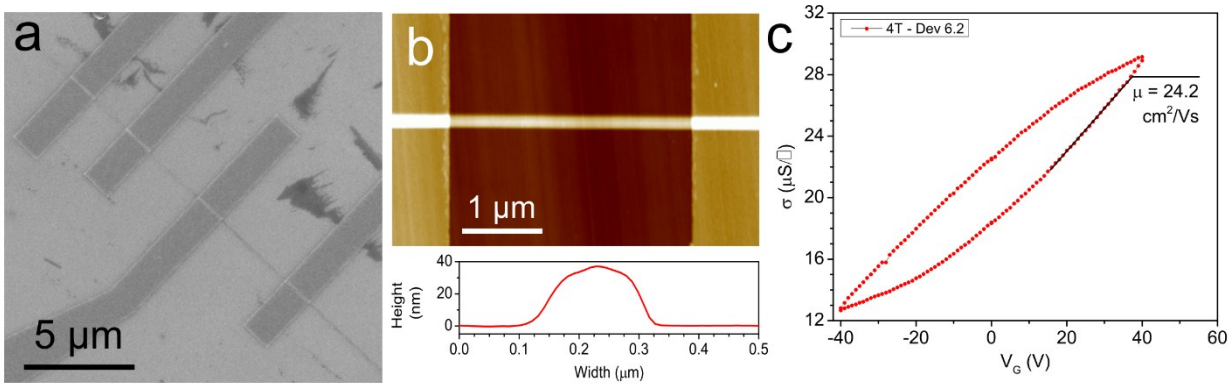

Figure S4. (a) SEM image of a multiterminal TiS_3 device. **(b)** AFM image of the TiS_3 nanoribbon connecting two inner Cr/Au electrode is (a). **(c)** Representative height profile measured across the TiS_3 nanoribbon shown in (b). **(d)** Conductivity (σ) – gate voltage (V_G) dependence for the TiS_3 device shown in (a) measured by four-point probe method.

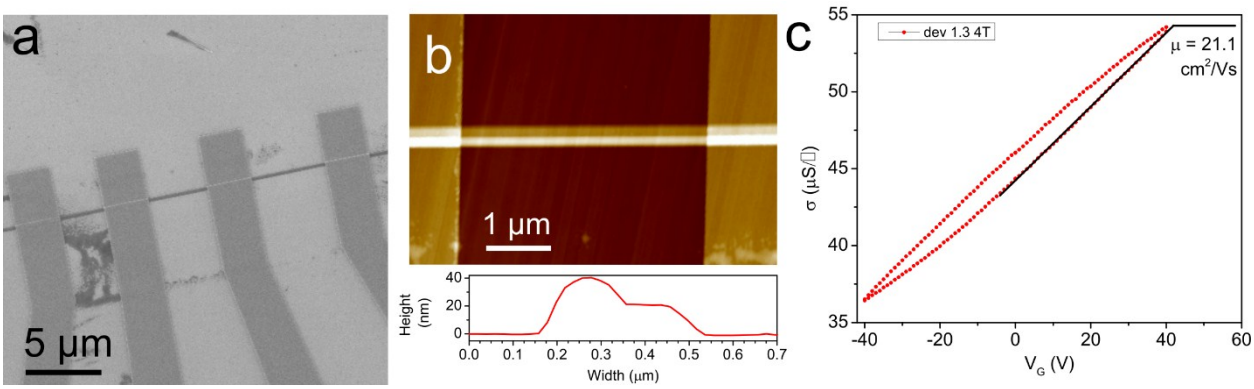

Figure S5. (a) SEM image of a multiterminal TiS_3 device. **(b)** AFM image of the TiS_3 nanoribbon connecting two inner Cr/Au electrode is (a). **(c)** Representative height profile measured across the TiS_3 nanoribbon shown in (b). **(d)** Conductivity (σ) – gate voltage (V_G) dependence for the TiS_3 device shown in (a) measured by four-point probe method.

7. Effect of Al_2O_3 ALD on electronic properties of TiS_3 FETs

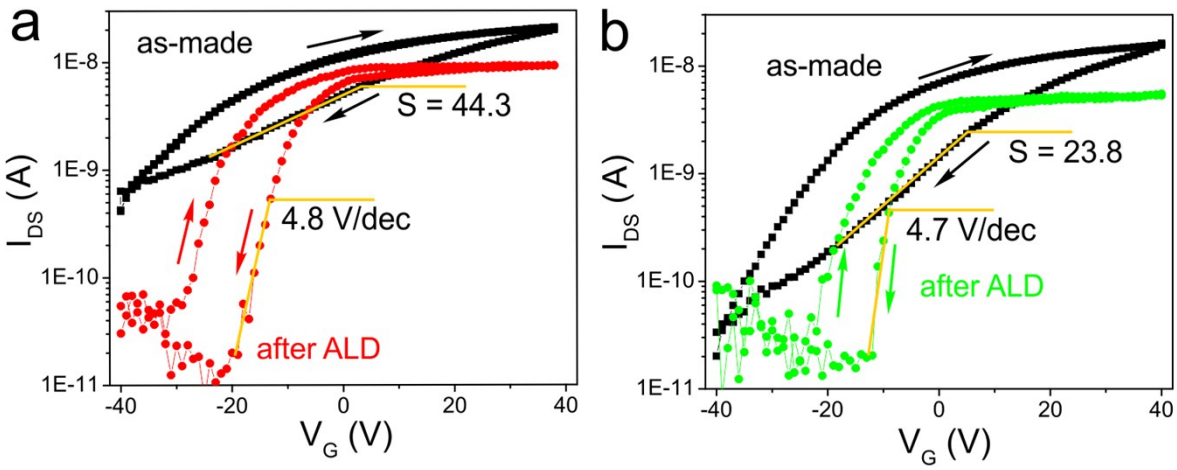

c

Device #	Subthreshold swing, S (V/dec)	
	as-made	after ALD
1	38.21	4.49
2	44.30	4.83
3	23.78	4.68
4	19.13	3.42

Figure S6. ALD of Al_2O_3 on TiS_3 FETs. For all measurements V_{DS}= 0.1 V. **(a,b)** Comparison of the drain-source current (I_{DS}) – gate voltage (V_G) dependencies for (a) TiS_3 device #2 and (b) TiS_3 device #3 before and after ALD of Al_2O_3. **(c)** Comparison of the subthreshold swing (S) values for all four devices (see Figure S3) before and after ALD of Al_2O_3.